Commun. Math. Phys. 257, 303–317 (2005)
Digital Object Identifier (DOI) 10.1007/s00220-004-1264-7

Communications in **Mathematical Physics**

Dynamic Scaling in Miscible Viscous Fingering

G. Menon[1], **F. Otto**[2]

[1] Division of Applied Mathematics, Brown University, Providence, RI 02912, USA. E-mail: menon@dam.brown.edu
[2] Institute for Applied Mathematics, University of Bonn, Wegelerstr. 10, Bonn 53115, Germany. E-mail: otto@iam.uni-bonn.de

Received: 17 May 2004 / Accepted: 4 July 2004
Published online: 12 February 2005 –

Abstract: We consider dynamic scaling in gravity driven miscible viscous fingering. We prove rigorous one-sided bounds on bulk transport and coarsening in regimes of physical interest. The analysis relies on comparison with solutions to one-dimensional conservation laws, and new scale-invariant estimates. Our bounds on the size of the mixing layer are of two kinds: a naive bound that is sharp in the absence of diffusion, and a more careful bound that accounts for diffusion as a selection criterion in the limit of vanishingly small diffusion. The naive bound is simple and robust, but does not yield the experimental speed of transport. In a reduced model derived by Wooding [20], we prove a sharp upper bound on the size of the mixing layer in accordance with his experiments. Wooding's model also provides an example of a scalar conservation law where the entropy condition is not the physically appropriate selection criterion.

1. Introduction

We study pattern formation and mixing generated by the gravity driven instability of an interface between two fluids in a porous medium. We may distinguish three stages in the evolution of the flow: (a) an early stage governed by the linear instability, (b) an intermediate stage with scaling behavior, and (c) a late stage. The linear stability analysis is classical [2, 9, 18] and describes the evolution in stage (a) well. The late stage (c) may be quite different depending on competing physical effects such as molecular diffusion or surface tension. Saffman and Taylor's discovery of a family of traveling wave solutions (fingers), parametrized by $\lambda \in [0, 1]$, has led to extensive work on finger selection [18]. Much of this work has been sophisticated linear stability and singular perturbation analyses examining the role of surface tension in selecting a finger (see [1, 19] for reviews). This analysis is directly related to the asymptotic profile (stage (c)) observed experimentally by Saffman and Taylor. It also provides a formal understanding of the stability of the coherent fingers in stage (b) . More precisely, it is assumed that even when there

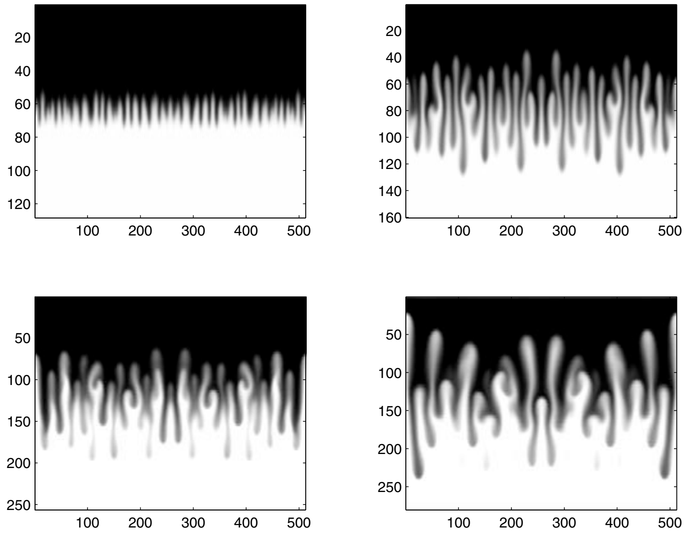

Fig. 1. Coarsening of fingers and bulk transport

are many competing fingers, these are locally described by the Saffman-Taylor solution, and one of these ($\lambda = 1/2$ typically) is selected by an additional physical mechanism.

In most experiments there is a broad range of active modes and in view of the instability, one may expect the evolution in stage (b) to be unpredictable. Yet experimental and numerical work shows that despite the unpredictability of fine details, certain statistics (size of the mixing layer, finger width) satisfy robust scaling laws. Little is known analytically about this fully nonlinear and physically interesting regime.

Our goal is to obtain rigorous results on dynamic scaling for the simplest nontrivial model problem. We simplify matters by considering the gravity driven transport of a dilute solute s by convection and diffusion (miscible fingering). Then one may assume that the mobility is uniform, and after suitable non-dimensionalization (see [20] for a derivation) we have the system

$$\partial_t s + \mathbf{u} \cdot \nabla s = \Delta s, \quad s \in [0, 1], \tag{1}$$

$$\nabla \cdot \mathbf{u} = 0, \tag{2}$$

$$\mathbf{u} + \nabla p = -s\mathbf{e}_z. \tag{3}$$

The domain is $x = (y, z) \in [0, L]^{n-1} \times \mathbb{R}$, $n = 2, 3$. Equation (3) is Darcy's law: the velocity is linearly proportional to the driving force which comprises a pressure gradient and buoyancy ($-s\mathbf{e}_z$). The Peclet number, L, is a measure of the strength of diffusion. It is the only external parameter. We are interested in scaling behavior that is independent of L and boundary effects, and in particular the behavior as $L \to \infty$. For convenience we use periodic boundary conditions in y. We consider initial conditions that are small perturbations of the flat unstable stratification. Figure 1 shows four snapshots of the evolution. After an initial transient, the system develops a mixing zone with an intricate network of fingers on a mesoscopic scale. The details of fingering are sensitive to intial data, but there is a remarkable statistical regularity observed in physical [20] and numerical experiments [10]:

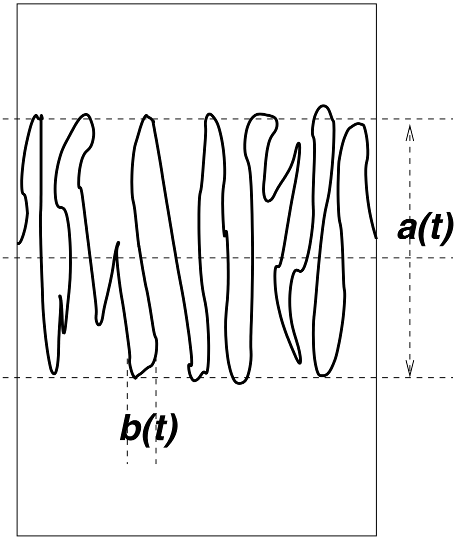

Fig. 2. Caricature of $a(t)$ and $b(t)$

(a) The end-to-end width of the mixing zone is independent of L for large L, and it is typically t.
(b) The fingers broaden at the rate $O(\sqrt{t})$.

Two features of these scaling laws are astonishing on closer inspection.

(a) *Diffusive slowdown* (or the missing factor of 2): The fastest exact solutions in the absence of diffusion (Saffman-Taylor fingers with $\lambda = 0$) have speed 1, and would give a mixing zone of size $2t$ (not t). In particular, all Saffman-Taylor solutions with $\lambda \in [0, 1/2)$ cannot be selected by a vanishing diffusion limit.
(b) Coarsening is limited by diffusion, but experiments and numerical simulations show it is primarily driven by the convective coalescence of nearby fingers. Thus, the $\sqrt{t}$ width of fingers is not based on transverse spreading by diffusion.

A rigorous formulation of dynamic scaling involves a definition of vertical and horizontal length scales (denoted $a(t)$ and $b(t)$ respectively as in Fig. 2), followed by upper and lower bounds of the form

$$1 - o(1) \leq \frac{a(t)}{t} \leq 1, \qquad c \leq \frac{b(t)}{\sqrt{t}} \leq C, \quad t \gg 1 \tag{4}$$

for some constants $C \geq c > 0$, under minimal assumptions on initial data. The estimates on a measure the size of the mixing zone, and the constant is crucial. The estimates on b are a statement about the rate of coarsening, and the constant is not as important. But in such generality, (4) is false: the unstable stratification s_0 (defined in (5) below), evolves diffusively without fingering. Therefore, for this solution $a(t) \sim \sqrt{t}$, and there is no coarsening since there are no fingers. We may use continuity in initial conditions to then construct solutions that coarsen arbitrarily slowly. It is a subtle problem to precisely eliminate such "unphysical" initial data using assumptions of genericity or randomness.

We sidestep this issue altogether, and focus on physically meaningful estimates that are simple, natural and robust. What we prove are upper bounds on the potential energy, mean perimeter, and mixing entropies that scale in the natural way with time. Though we obtain only one-sided estimates, these are robust and free of any ansatz on the structure of the flow. This perspective has been used profitably in a wide range of problems [4, 6, 12, 17], and is similar in spirit to the now classical work of Howarth [11].

2. Statement of Results

2.1. Definition of bulk quanitities. Let Q denote the spatial domain $x := (y, z) \in [0, L]^{n-1} \times \mathbb{R} := D \times \mathbb{R}$, $n = 2, 3$. We consider periodic boundary conditions in y. The unstable stratification

$$s_0(z) = \begin{cases} 0, & z < 0 \\ 1, & z \geq 0 \end{cases} \tag{5}$$

will serve as the main reference configuration. We are interested in estimates independent of the length scale L. It is thus natural to consider the horizontal average of a scalar field $f : Q \to \mathbb{R}$

$$\bar{f}(z) = \frac{1}{|D|} \int_D f(y, z)\, dy, \tag{6}$$

and normalized integrals of the form

$$⨍ f\, dx := \int_{\mathbb{R}} \frac{1}{|D|} \int_D f(y, z)\, dy\, dz = \int_{\mathbb{R}} \bar{f}\, dz. \tag{7}$$

The gravitational potential energy of $s(t, x)$ is defined by

$$E(t) = ⨍ (s_0(z) - s(t, x))\, z\, dx = \int_{\mathbb{R}} (s_0(z) - \bar{s}(t, z))\, z\, dz. \tag{8}$$

To be more precise, E is the negative of the gravitational energy. Observe that since $s \in [0, 1]$ we have $E \geq 0$, and $E = 0$ if and only if $s = s_0$. E is also a measure of mass transported, and we shall define $a = 2\sqrt{6E}$ (the choice of constant is explained in Remark 1 below). In order to measure the width of fingers, we define the mean perimeter

$$P(t) = ⨍ |\nabla s(t, x)|\, dx = \int_0^1 \mathcal{H}^{n-1}[s^{-1}(c)]\, dc. \tag{9}$$

The second inequality is the co-area formula ([21, Thm 2.7.1]) and justifies the terminology mean perimeter. One effect of diffusion is to smooth sharp transitions and create "mushy zones" where $0 < s < 1$. The size of these mixing zones can be measured by "mixing entropies" that vanish in the pure phases where $s \in \{0, 1\}$. We will work mainly with the entropies

$$H(t) = ⨍ s(1 - s)\, dx, \quad S(t) = -⨍ (s \log s + (1 - s) \log(1 - s))\, dx. \tag{10}$$

2.2. Uniform estimates on bulk quantities. The following estimates are independent of L and provide an upper bound on $a(t)$ and a lower bound on $b(t)$.

Theorem 1. *Let $s(t,x)$ be a classical solution to (1)–(3), with energy $E(t)$, mixing entropy $H(t)$, and perimeter $P(t)$. Then*

$$\limsup_{t\to\infty} \frac{E(t)}{t^2} \le \frac{1}{6}, \quad \limsup_{t\to\infty} \frac{H(t)}{t} \le \frac{1}{3}, \tag{11}$$

and

$$\limsup_{t\to\infty} \frac{1}{t^2} \int_0^t P^2(\tau)d\tau \le \frac{\pi}{9}. \tag{12}$$

Remark 1. In a loose sense, the energy estimate (11) bounds $s(t,x)$ by comparison to the rarefaction wave (entropy solution) to the following Riemann problem:

$$\partial_t s_u - \partial_z(s_u(1-s_u)) = 0, \quad s_u(0,z) = s_0(z). \tag{13}$$

More explicitly, $s_u(t,z) = s^*(z/t)$, where

$$s^*(\xi) = \begin{cases} 0 & \xi < -1, \\ \frac{1+\xi}{2} & -1 \le \xi \le 1, \\ 1 & \xi > 1. \end{cases} \tag{14}$$

Thus, the end-to-end size of the mixing zone is $a(t) = 2t$. The energy associated to the profile $s_u(t,z)$ is $E(t) = t^2/6 = a^2/24$. A similar (and more general) comparison of $s(t,x)$ with an entropy solution for a suitable Riemann problem appears in earlier work by one of the authors [16]. However, notice that the estimate $a(t) \le 2t$ is twice the experimental result $a(t) \le t$. Here our interest is in understanding this unexpected gap.

Remark 2. Estimate (12) is an integrated version of the (unproven) pointwise inequality

$$P(t) \le \frac{\sqrt{2\pi t}}{3}. \tag{15}$$

More precisely, the largest C and α in a scaling ansatz $P(t) = Ct^\alpha$ compatible with (12) are the values in (15). The bound on α may be interpreted as a lower bound on the width of fingers as follows. If we assume the typical form of s is as shown in Fig. 2, we see that

$$P(t) \approx \fint |\partial_y s|\, dx \approx \int_{|z|\le a/2} N(z)\, dz = a\bar{N} = \frac{a}{b}, \tag{16}$$

where $N(z)$ is the number of fingers per unit width on any horizontal level $z = \text{const}$, $\bar{N}$ is the mean number of fingers, and $b = 1/\bar{N}$ is the mean wavelength of fingers. The upper estimate (15) now yields,

$$b(t) \ge \frac{a(t)}{P(t)} \ge \frac{3\sqrt{t}}{\sqrt{2\pi}} \tag{17}$$

if $a(t) = t$. It is in this weak (but also robust) sense, that (12) is an estimate on coarsening.

2.3. Sharp pointwise estimates in a reduced model. The crux of the problem is the focusing mechanism of convection and the subtle role of diffusion in arresting singularity formation. This is manifested experimentally as diffusive slowdown. A similar phenomenon is seen experimentally and numerically in the Rayleigh-Taylor instability [5, 7] though this is harder to analyze. The scaling $a(t) \sim Ct$ (or $a(t) \sim Ct^2$ for the Rayleigh-Taylor instability) is clear on physical grounds. However, deeper insight is needed to find the sharp constant (the terminal speed or acceleration in experiments). We have been unable to improve Theorem 1 for the system (1–3) or to formulate an appropriate result on singularity formation. However, the following reduced 2-d model derived by Wooding [20] is more tractable to analysis:

$$\partial_t s + \mathbf{u} \cdot \nabla s = \Delta s, \quad s \in [0, 1], \tag{18}$$

$$\nabla \cdot \mathbf{u} = 0, \tag{19}$$

$$\mathbf{u} = (v, w), \quad w = \bar{s} - s. \tag{20}$$

Equation (20) is formally obtained from Darcy's law when the horizontal and vertical scales separate ($a(t) \gg b(t)$). Equations (2) and (3) imply

$$\triangle w = -\partial_y^2 s.$$

If the height of fingers is much greater than their width ($a(t) \gg b(t)$), it is natural to assume $|\partial_y^2 w| \gg |\partial_z^2 w|$, and formally we have

$$\partial_y^2 w = -\partial_y^2 s,$$

which is integrated to yield (20) (see [20] for details). The proof of Theorem 1 extends to the reduced system, and we have as before

Theorem 2. *Let $s(t, x)$ be a classical solution to (18)–(20), with energy $E(t)$, mixing entropy $H(t)$, and perimeter $P(t)$. Then*

$$\limsup_{t\to\infty} \frac{E(t)}{t^2} \leq \frac{1}{6}, \quad \limsup_{t\to\infty} \frac{H(t)}{t} \leq \frac{1}{3}, \quad \limsup_{t\to\infty} \frac{1}{t^2} \int_0^t P^2(\tau)d\tau \leq \frac{\pi}{9}. \tag{21}$$

Theorem 2 is completely analogous to Theorem 1, and suggests the mixing zone grows as $a(t) = 2t$. But this is false.

Theorem 3. *Let $s(t, x)$ be a classical solution to (18)–(20) with continuous initial data $s(0, x) : Q \to [0, 1]$ such that*

$$\lim_{z\to-\infty} \max_y s(y, z) = 0, \quad \lim_{z\to\infty} \min_y s(y, z) = 1. \tag{22}$$

Then for any $c > \frac{1}{2}$,

$$\lim_{t\to\infty} \max_y s(t, y, -ct) = 0, \quad \lim_{t\to\infty} \min_y s(t, y, ct) = 1. \tag{23}$$

Remark 3. The pointwise estimates (23) show that the mixing zone does not spread faster than $a(t) = t$ under mild localization assumptions on the initial data (22). Numerical calculations suggest that this estimate is sharp [15, p.88]. The mean speed of the finger tips in Wooding's experiments is 0.446, or $a(t) = 0.892t$ [20, Eq.15].

Remark 4. The slowdown of the finger speed by a factor of $1/2$ is reminescent of finger selection by surface tension [19], and it is natural to say, the Saffman-Taylor finger of width $\lambda = 1/2$ is selected by diffusion. However, we stress that Theorem 3 is free of any assumptions on the structure of the solutions except for the localization assumption (22).

2.4. Connections with scalar conservation laws. The connections with the Riemann problem (13) may be clarified further for the reduced model (18)–(20). Let us first neglect the effect of diffusion and formally pass to the sharp interface limit $s \in \{0, 1\}$ *a.e.* We drop $\triangle s$ in (18), and substitute for w from (20), to obtain

$$\partial_t s + \partial_y(vs) + \partial_z((\overline{s} - s)s) = 0. \tag{24}$$

Equation (24) possesses a remarkable closure property. In the absence of diffusion, the pointwise constraint $s \in \{0, 1\}$ *a.e.* is preserved. Thus, when we average in y we find

$$\overline{ws} = \overline{(\overline{s} - s)s} = \overline{s}^2 - \overline{s^2} = \overline{s}^2 - \overline{s}, \tag{25}$$

since nonlinearity *does* commute with averaging if $s \in \{0, 1\}$ *a.e.* Since we are considering small perturbations of the flat interface, it is natural to choose initial data $\overline{s}(0, z) = s_0(z)$. In this formal limit, the evolution of $\overline{s}$ is determined by the Riemann problem

$$\partial_t \overline{s} - \partial_z\left(\overline{s}(1 - \overline{s})\right) = 0, \quad \overline{s}(0, z) = s_0(z). \tag{26}$$

The entropy solution to this Riemann problem is the rarefaction wave in (14). But this is ruled out by Theorem 3. In fact, the proof of Theorem 3 suggests that the physically appropriate self-similar weak solution to (13) is $\overline{s}(t, z) = s^{\#}(z/t) := s^{\#}(\xi)$, where

$$s^{\#}(\xi) = \begin{cases} 0 & \xi < -\frac{1}{2}, \\ \frac{1}{2} & -\frac{1}{2} \le \xi \le \frac{1}{2}, \\ 1 & \xi > \frac{1}{2}. \end{cases} \tag{27}$$

The main heuristic idea behind the proof of Theorem 3 is that there is always a sharp gradient at the fingertips. This is made precise by comparing solutions of (18)–(20)) to viscous shocks of Burgers equation. Thus the physically appropriate solution to (14) consists of two "unphysical" shocks propagating outwards at speed 1/2 (unphysical meaning that the shocks fail to satisfy Lax's entropy condition, [13, p.9]).

3. Proof of Bulk Estimates

3.1. Main lemmas. Theorem 1 is based on energy balance, control of gradients using mixing entropies, and an interpolation argument linking the mixing entropies and energy. We formalize these ideas in the following lemmas.

Lemma 1 (Energy balance). *Let $s(t, x)$ be a classical solution to Eqs. (1)–(3) with energy $E(t)$ and mixing entropy $H(t)$. Then*

$$\dot{E} = \int_{\mathbb{R}} \overline{s}(1 - \overline{s})\, dz - H(t) - ⨍ |\nabla p|^2\, dx + 1. \tag{28}$$

Lemma 2 (Growth of mixing entropies). *Let $s(t, x)$ be a classical solution to (1)–(3) with mixing entropies H and S. Then*

$$\dot{H} = 2 ⨍ |\nabla s|^2\, dx, \quad \dot{S} = ⨍ \frac{|\nabla s|^2}{s(1 - s)}\, dx. \tag{29}$$

Lemma 3 (Interpolation). *Let $\bar{s} : \mathbb{R} \to [0,1]$ be measurable and let $E = \int_{\mathbb{R}} (s_0 - \bar{s})\, z\, dz$. Then*

$$\int_{\mathbb{R}} \bar{s}(1-\bar{s})\, dz \le \sqrt{\frac{2E}{3}}, \tag{30}$$

$$-\int_{\mathbb{R}} \left(\bar{s}\log\bar{s} + (1-\bar{s})\log(1-\bar{s})\right)\, dz \le \pi\sqrt{\frac{2E}{3}}. \tag{31}$$

3.2. Proof of Theorem 2. We combine Lemma 1 and Lemma 3 to obtain,

$$\dot{E} \le \int_{\mathbb{R}} \bar{s}(1-\bar{s})\, dz + 1 \le \sqrt{\frac{2E}{3}} + 1. \tag{32}$$

This estimate may be integrated to yield (11). The details are as follows. Let $e(t)$ solve

$$\dot{e} = \sqrt{\frac{2e}{3}} + 1, \quad e(0) = E(0). \tag{33}$$

We may integrate (33) explicitly to obtain the solution

$$\sqrt{\frac{2e(t)}{3}} - \sqrt{\frac{2e(0)}{3}} - \log\left(\frac{\sqrt{2e(t)/3}+1}{\sqrt{2e(0)/3}+1}\right) = \frac{t}{3}. \tag{34}$$

We claim that for every $t \ge 0$,

$$E(t) \le e(t). \tag{35}$$

Indeed, if $\varepsilon > 0$ let $e_\varepsilon(t)$ be the solution to (33) with $e_\varepsilon(0) = E(0) + \varepsilon$. We combine (32) and (33) and integrate to obtain

$$e_\varepsilon(t) - E(t) \ge \varepsilon + \sqrt{\frac{2}{3}}\int_0^t \left(\sqrt{e_\varepsilon(\tau)} - \sqrt{E(\tau)}\right) d\tau.$$

Let $T = \inf\{t \ge 0 : e_\varepsilon(t) < E(t)\}$. We claim that $T = \infty$. Since $\varepsilon > 0$ we have $T > 0$. If T is finite, then we have $e_\varepsilon(T) = E(T)$, which implies the contradiction $0 \ge \varepsilon > 0$. This proves (35). To estimate H, we observe that

$$\int_{\mathbb{R}} \bar{s}(1-\bar{s})\, dz - H(t) = ⨍ \left(\bar{s}(1-\bar{s}) - s(1-s)\right)\, dx = ⨍ (s-\bar{s})^2\, dx \ge 0.$$

Thus, we apply Lemma 3 again to find

$$H(t) \le \int_{\mathbb{R}} \bar{s}(1-\bar{s})\, dz \le \sqrt{\frac{2E(t)}{3}}. \tag{36}$$

The estimate (11) now follows from (34), (35), and (36). To prove (12) we apply the Cauchy-Schwarz inequality and (29) to obtain,

$$P(t) = ⨍ |\nabla s| \le \left(⨍ s(1-s)\right)^{1/2}\left(⨍ \frac{|\nabla s|^2}{s(1-s)}\right)^{1/2} = H^{1/2}(\dot{S})^{1/2}. \tag{37}$$

We integrate in time to obtain

$$\int_0^t P^2(\tau)d\tau \le \int_0^t H(\tau)\dot{S}(\tau)d\tau \le H(t)S(t) \le \frac{2\pi}{3}E(t). \tag{38}$$

In the second inequality we have used the monotonicity of H and S. In the third inequality we used (30) and (31). We combine (38) and (11) to obtain (12). This completes the proof of Theorem 1.

3.3. Proof of Lemma 1. Lemma 1 is a statement of energy balance. For any scalar field $\tilde{s} : \mathbb{R} \to \mathbb{R}$ ($\tilde{s} = \tilde{s}(z)$) such that $s - \tilde{s} \in L^2(Q)$ the elliptic system

$$\nabla \cdot \mathbf{u} = 0, \quad \mathbf{u} + \nabla \tilde{p} = (\tilde{s} - s)\mathbf{e}_z$$

is a Helmholtz decomposition of the vector field $(\tilde{s} - s)\mathbf{e}_z$, and we have the orthogonality relations

$$⨍ |\mathbf{u}|^2\,dx + ⨍ |\nabla \tilde{p}|\,dx = ⨍ (s - \tilde{s})^2\,dx, \quad ⨍ \mathbf{u} \cdot \nabla \tilde{p}\,dx = 0. \tag{39}$$

Observe that there is no convection unless s oscillates in y: if $s(y, z) = s(z)$, then $\mathbf{u} = \mathbf{0}$. The velocity $\mathbf{u}$ is uniquely determined by s, but $\tilde{p}$ depends on the background field $\tilde{s}$. We choose $\tilde{s} = \bar{s}$ to obtain

$$\begin{aligned} ⨍ |\mathbf{u}|^2\,dx &= ⨍ (s - \bar{s})^2\,dx - ⨍ |\nabla p|^2\,dx \\ &= \int_{\mathbb{R}} \bar{s}(1 - \bar{s})dz - ⨍ s(1 - s)\,dx - ⨍ |\nabla p|^2\,dx. \end{aligned} \tag{40}$$

We substitute (8) in (1), integrate by parts, and use (3), (39) and the boundary conditions to find

$$\dot{E} = -⨍ s\mathbf{e}_z \cdot \mathbf{u}\,dx + ⨍ \nabla s \cdot \mathbf{e}_z\,dx = ⨍ |\mathbf{u}|^2\,dx + 1. \tag{41}$$

Lemma 1 follows from (40) and (41).

3.4. Proof of Lemma 2. Lemma 2 is a particular consequence of the growth of concave entropies. Let $g : [0, 1] \to [0, \infty)$ be a smooth concave function such that $g(0) = g(1) = 0$. Let $s(t, x)$ be a classical solution to (1). We multiply Eq. (1) by $g'(s)$ and integrate to obtain

$$\frac{d}{dt} ⨍ g(s(t, x))\,dx = -⨍ \nabla \cdot (g(s)\mathbf{u})\ dx - ⨍ g'(s)\nabla \cdot \nabla s\,dx = -⨍ g''(s)|\nabla s|^2\,dx,$$

after integration by parts.

3.5. Proof of Lemma 3. Lemma 3 is a corollary of the following general scale-invariant interpolation inequality.

Theorem 4. *Assume $g : [0,1] \to [0,\infty)$ is a concave, symmetric (that is $g(s) = g(1-s)$) entropy that satisfies the growth condition*

$$g(s) \leq C_\alpha s^\alpha, \quad \textit{for} \quad \textit{some} \quad \alpha > \frac{1}{2}. \tag{42}$$

Then if $s : \mathbb{R} \to [0,1]$ is measurable we have

$$\int_{\mathbb{R}} g(s(z))\,dz \leq C_g \left(\int_{\mathbb{R}} (s_0 - s) z\,dz \right)^{1/2} = C_g E^{1/2}. \tag{43}$$

The sharp constant C_g is given by

$$C_g = \left(2 \int_0^1 g'(s)^2\,ds \right)^{1/2}. \tag{44}$$

The inequality is strict unless $s(z) = s_g(z/t)$ for some $t > 0$, where $s_g(\xi)$ is the optimal profile defined implicitly by

$$g'(s_g(\xi)) = \xi, \quad \xi \in \mathbb{R}. \tag{45}$$

Remark 5. A growth condition such as (42) is necessary. If $g = \sqrt{s(1-s)}$ we may consider a profile such that $|s - s_0| = (|z| \log |z|)^{-2}$ for large z. Then E is finite, but $\int_{\mathbb{R}} g(s)dz$ is not.

Remark 6. The optimal profiles in (45) are the rarefaction waves (entropy solutions) to the following Riemann problem:

$$\partial_t s - \partial_z(g(s)) = 0, \quad s(0,z) = s_0(z).$$

If $g = s(1-s)$, then $C_g = \sqrt{2/3}$ and the optimal profile is the linear rarefaction wave in (14). If $g = -(s \log s + (1-s)\log(1-s))$, $C_g = \pi\sqrt{2/3}$.

Proof. 1. Symmetrization. Given $s : \mathbb{R} \to [0,1]$ define its symmetrization

$$s_{symm}(z) = \frac{1}{2}\left(s(z) + 1 - s(-z) \right). \tag{46}$$

Observe that s_{symm} is symmetric about the origin in the sense that

$$s_{symm}(z) = 1 - s_{symm}(-z). \tag{47}$$

E is unchanged under symmetrization, that is

$$\int_{\mathbb{R}} (s_0 - s_{symm})\, z\,dz = \int_{\mathbb{R}} (s_0 - s)\, z\,dz. \tag{48}$$

On the other hand, since g is concave and symmetric we have

$$g(s_{symm}(z)) \geq \frac{1}{2}\left(g(s(z)) + g(1 - s(-z)) \right) = \frac{1}{2}\left(g(s(z)) + g(s(-z)) \right).$$

Therefore,

$$\int_{\mathbb{R}} g(s_{symm}(z))\, dz \geq \int_{\mathbb{R}} g(s(z))\, dz. \tag{49}$$

2. Rearrangement. We now consider the increasing rearrangement s_{rearr} of s_{symm}. Rearrangement does not change the distribution function of s_{symm} ([14, Ch.3]) and we have

$$\int_{\mathbb{R}} g(s_{rearr}(z))\, dz = \int_{\mathbb{R}} g(s_{symm}(z))\, dz. \tag{50}$$

On the other, rearrangement decreases the potential energy. This is easily seen when s_{symm} is a simple function, and the general case follows by approximation.
3. Henceforth, we will suppose that $s(z) = s_{rearr}(z)$. We will first show that there is some constant C such that $\int_{\mathbb{R}} g(s)ds \leq CE^{1/2}$ and then find the sharp constant and optimal profile. In the following, C denotes a constant that depends only on α and g that may increase from line to line. By the symmetry of s and g it suffices to consider $\int_{-\infty}^{0} g(s(z))dz$. Let $\theta > 0$. We then have

$$\begin{aligned}
\int_{-\infty}^{0} g(s(z))dz &= \int_{-\theta}^{0} g(s(z))dz + \int_{-\infty}^{-\theta} g(s(z))dz \\
&\leq \theta\|g\|_\infty + C\int_{-\infty}^{-\theta} s^\alpha(z)dz \\
&\leq \theta\|g\|_\infty + C\left(\int_{-\infty}^{0} |z|s(z)dz\right)^\alpha \left(\int_{-\infty}^{-\theta} |z|^{-\alpha/(1-\alpha)}dz\right)^{1-\alpha} \\
&\leq \theta\|g\|_\infty + CE^\alpha\theta^{1-2\alpha}.
\end{aligned} \tag{51}$$

We optimize and substitute $\theta = \|g\|_\infty^{-1/2\alpha} E^{1/2}$ in (51) to obtain

$$\int_{\mathbb{R}} g(s(z))dz \leq C\|g\|_\infty^{1-1/2\alpha} E^{1/2}. \tag{52}$$

4. The best profile and constant: The sharp constant is

$$C_g = \sup_s \frac{\int_{\mathbb{R}} g(s(z))\, dz}{E^{1/2}}, \tag{53}$$

where the supremum is taken over all $s : \mathbb{R} \to [0, 1]$ measurable. As we have seen, we may restrict attention to increasing, symmetric s. In this case, we may identify s as a probability distribution function, and consider Lebesgue-Stieltjes integrals with respect to the positive measure $s(dz)$ [8]. We will now consider the right inverse of $s(z)$ written as $z(s)$. Then we have

$$E = \int_{\mathbb{R}} (s_0 - s(z))\, z\, dz = \int_{\mathbb{R}} \frac{z^2}{2}\, s(dz) = \frac{1}{2}\int_0^1 (z(s))^2\, ds. \tag{54}$$

Moreover, we may also write

$$\int_{\mathbb{R}} g(s(z))\, dz = \int_0^1 g(s)\frac{dz}{ds}\, ds = -\int_0^1 g'(s)z(s)\, ds.$$

It follows from the Cauchy-Schwarz inequality and (54) that

$$\int_{\mathbb{R}} g(s(z))\,dz \leq \left(\int_0^1 g'(s)^2\,ds\right)^{1/2} \left(\int_0^1 (z(s))^2\,ds\right)^{1/2} = \left(2E\int_0^1 g'(s)^2\,ds\right)^{1/2}.$$

The inequality is sharp if and only if $z(s) = tg'(s)$ for some $t > 0$. □

4. Diffusive Slowdown

4.1. Bulk estimates and diffusion. The upper estimate $a(t) \leq 2t$ in Theorem 1 does not account for the effect of diffusion. The same estimate is obtained if we neglect diffusion, and rewrite Eq. (1) as

$$\partial_t s + \mathbf{u}\cdot\nabla s = 0.$$

Mass is now transported only by convection, and (41) changes to $\dot{E} = ⨍|\mathbf{u}|^2$. We now use (40) to obtain

$$\dot{E} = \int_{\mathbb{R}} \bar{s}(1-\bar{s})\,dz - H - ⨍|\nabla p|^2 \leq \sqrt{\frac{2E}{3}}, \tag{55}$$

which we integrate to obtain $E(t) \leq t^2/6$ as earlier. Moreover, this naive upper bound is sharp if we consider a weak solution obtained as the limit of a periodic array of Saffman-Taylor fingers. A similar analysis on the reduced model (18)–(19) yields the analogous (and simpler) estimate

$$\dot{E} = ⨍(s-\bar{s})^2\,dx = \int_{\mathbb{R}} \bar{s}(1-\bar{s})dz - H \leq \sqrt{\frac{2E}{3}}. \tag{56}$$

One effect of diffusion is to produce molecularly mixed "mushy zones" where $0 < s < 1$. If these zones are sufficiently large, then they act as drags on the bulk motion. More precisely, the existence of lower bounds of the form

$$\liminf_{t\to\infty} \frac{H(t)}{t} \geq c, \quad \text{or} \quad \liminf_{t\to\infty} ⨍|\nabla s|^2\,dx \geq c, \tag{57}$$

for some $c > 0$, coupled with (28) shows that $\limsup_{t\to\infty} 6E/t^2 < 1$ (strict inequality). However, neither inequality in (57) is true in full generality (initial data s_0 serves as a counterexample again). We have been unable so far to prove diffusive slow down in (1)–(2) by this argument. It is worth noting that obtaining similar bounds is a key obstruction in mathematical studies of turbulence [3, Sect. 3]. Nevertheless, the estimates in (57) provide a valuable heuristic hint about the role of gradients and diffusion.

4.2. Proof of Theorem 3. We construct upper and lower solutions that bound the spreading of solutions to (18)–(20). The main heuristic idea is the gradients are always sharp at fingertips. This suggests comparing $s(t,x)$ with a suitable viscous shock profile. By the symmetry of the problem, it suffices to bound the downward spreading by an upper solution. The upper solutions are viscous shock profiles for Burgers equation (more precisely, Burgers equation with a *concave* flux $-s^2/2$), that is

$$\partial_t s_* - \partial_z \left(\frac{s_*^2}{2}\right) = \partial_z^2 s_*. \tag{58}$$

We consider viscous shocks that connect the states $\varepsilon > 0$ and $1+\varepsilon$ at $\mp\infty$ respectively. $\varepsilon > 0$ may be chosen arbitrarily small. The viscous shock profiles are found by making the traveling wave ansatz $s_*(t,x) = s_\varepsilon(z + c_\varepsilon t) := s_\varepsilon(\zeta)$ in (58). The only admissible speed c_ε is determined by the Rankine-Hugoniot condition,

$$c_\varepsilon = \frac{1}{2}\frac{(1+\varepsilon)^2 - \varepsilon^2}{1+\varepsilon-\varepsilon} = \frac{1}{2} + \varepsilon. \tag{59}$$

The shock profiles solve the differential equation

$$\frac{ds_\varepsilon}{d\zeta} = \frac{1}{2}\left(1+\varepsilon - s_\varepsilon\right)\left(s_\varepsilon - \varepsilon\right). \tag{60}$$

Thus, s_ε is strictly increasing and given explicitly by

$$s_\varepsilon(\zeta) = \varepsilon + \frac{1}{2}\left(1 + \tanh\left(\frac{\zeta - z_0}{4}\right)\right), \tag{61}$$

where z_0 is an arbitrary constant that reflects the invariance of (58) under translations in z. In order to find lower solutions, we transform (58) under the symmetry $s_* \to 1 - s_*$, $z \to -z$, to obtain,

$$\partial_t(1-\tilde{s}_*) + \partial_z\left(\frac{(1-\tilde{s}_*)^2}{2}\right) = \partial_z^2(1-\tilde{s}_*). \tag{62}$$

The viscous shock profile that connects the states ε, $1+\varepsilon$ at $\mp\infty$ is $\tilde{s}_*(t,x) = s_\varepsilon(z - c_\varepsilon t)$. The speed c_ε and profile s_ε are given by (59) and (61) respectively. Theorem 3 now follows from the following lemma.

Lemma 4. *Assume $s(t,x)$ is a classical solution to (18)–(19) with continuous initial data $s(0,x)$.*

(a) If $s(0,x) < s_*(0,x)$, then $s(t,x) < s_*(t,x)$ for all $t \geq 0$.
(b) Similarly, if $s(0,x) > \tilde{s}_*(0,x)$, then $s(t,x) > \tilde{s}_*(t,x)$ for all $t \geq 0$.

Proof (of Theorem 3). Fix $c > 1/2$. Let ε be arbitrary with

$$0 < \varepsilon \leq \frac{1}{2}\left(c - \frac{1}{2}\right).$$

Then by (59)

$$c - c_\varepsilon \geq \varepsilon > 0. \tag{63}$$

Since $\lim_{z\to-\infty} \max_y s(0, y, z) = 0$, we may choose z_0 in (61) such that $s(0, x) < s_*(0, x)$ for all x. By Lemma 4 we then have

$$s(t, y, -ct) < s_*(t, -ct) = s_\varepsilon((c_\varepsilon - c)t).$$

In view of (61) and (63), this yields

$$\limsup_{t\to\infty} \max_y s(t, y, -ct) \leq \varepsilon.$$

Since ε was arbitrary, we obtain as desired

$$\lim_{t\to\infty} \max_y s(t, y, -ct) = 0.$$

The proof of the lower estimate in (23) is similar, and is omitted. □

Proof (of Lemma 4). The proof is a direct application of the maximum principle. We write (18) in non-divergence form

$$\partial_t s + v\partial_y s + (\overline{s} - s)\partial_z s - \triangle s = 0, \tag{64}$$

and compare it with (58) rewritten as

$$\partial_t s_* + v\partial_y s_* + (\overline{s} - s_*)\partial_z s_* - \triangle s_* = \overline{s}\partial_z s_*. \tag{65}$$

Let $\theta = s_* - s$. We subtract (64) from (65), and rearrange terms to obtain

$$\partial_t \theta + v\partial_y \theta + w\partial_z \theta - \theta\partial_z s_* - \triangle\theta = \overline{s}\partial_z s_*. \tag{66}$$

We notice that by the strong maximum principle for (18) we have $s > 0$ for $t > 0$ and thus also $\overline{s} > 0$ for $t > 0$. On the other hand, $\partial_z s_* > 0$ as can be seen from (61). Hence the r. h. s. of (66) is strictly positive

$$\overline{s}\partial_z s_* > 0 \quad \text{for } t > 0. \tag{67}$$

We now argue by the maximum principle. Assume $\theta \geq 0$ was not true. Since $\theta(0, x) \geq 0$ and $\lim_{z\to\pm\infty} \theta(t, y, z) = \varepsilon$ uniformly in (t, y), there exists a $(t_*, x_*) \in (0, \infty) \times \mathbb{R}^2$ such that

$$\theta(t_*, x_*) = 0 \quad \text{and} \quad \theta(t, x) \geq 0 \ \ \forall (t, x) \in (0, t_*) \times \mathbb{R}^2.$$

In particular,

$$\partial_t \theta(t_*, x_*) = \partial_y \theta(t_*, x_*) = \partial_z \theta(t_*, x_*) = 0 \quad \text{and} \quad \triangle\theta(t_*, x_*) \geq 0. \tag{68}$$

Hence by (66) we would obtain $\overline{s}\partial_z s_*(t_*, x_*) \leq 0$ — in contradiction to (67). The proof of the lower estimate is identical. Redefine $\theta = s - \tilde{s}_*$. We then have

$$\partial_t \theta + v\partial_y \theta + w\partial_z \theta - \theta\partial_z \tilde{s}_* - \triangle\theta = (1 - \overline{s})\partial_z \tilde{s}_*, \tag{69}$$

and (68) holds again at a point of minimum. □

Acknowledgement. This work was supported by NSF DMS 03-05985, SFB 611 of the German Science Foundation at the University of Bonn, and the Max Planck Institute for Mathematics in the Sciences, Leipzig. G.M. acknowledges with pleasure the hospitality of the University of Bonn, and the MPI, Leipzig. F.O. acknowledges partial support through SFB 611.

References

1. Batchelor, G.K., Moffatt, H.K., Worster, M.G., eds.: *Perspectives in fluid dynamics*. Cambridge: Cambridge University Press, 2000
2. Chouke, R., van Meurs P., van der Poel, C.: The instability of slow, immiscible, viscous liquid-liquid displacements. Trans. AIME **216**, 188–194 (1958)
3. Constantin, P.: Some open problems and research directions in the mathematical study of fluid dynamics. In: *Mathematics Unlimited—2001 and beyond*, Berlin: Springer, 2001, pp. 353–360
4. Constantin, P., Kiselev, A., Oberman, A., Ryzhik, L.: Bulk burning rate in passive-reactive diffusion. Arch. Ration. Mech. Anal. **154**, 53–91 (2000)
5. Dimonte, G.: Nonlinear evolution of the Rayleigh-Taylor and Richtmyer-Meshkov instabilities. Physics of Plasmas, **6**, 2009–2015 (1999)
6. Doering, C.R., Constantin, P.: Bounds for heat transport in a porous layer. J. Fluid Mech. **376**, 263–296 (1998)
7. George, E., Glimm, J., Li, X.-L., Marchese, A., Xu, Z.-L.: A comparison of experimental, theoretical and numerical simulation of Rayleigh-Taylor mixing rates. PNAS **99**, 2587–2592 (2002)
8. Feller, W.: An introduction to probability theory and its applications. Vol. **II**. Second edition, New York: John Wiley & Sons Inc., 1971
9. Hill, S.: Channelling in packed columns. Chem. Eng. Sci. **1**, 247–253 (1952)
10. Homsy, G.M.: Viscous fingering in porous media. Ann. Rev. Fluid Mech. **19**, 271–311 (1987)
11. Howarth, L.N.: Bounds on flow quantities. Ann. Rev. Fluid. Mech. **4**, 1972
12. Kohn, R.V., Yan, X.: Upper bound on the coarsening rate for an epitaxial growth model. Comm. Pure Appl. Math. **56**, 1549–1564 (2003)
13. Lax, P.D.: Hyperbolic systems of conservation laws and the mathematical theory of shock waves. Philadelphia, Pa.: Society for Industrial and Applied Mathematics, 1973
14. Lieb, E.H., Loss, M.: *Analysis*. Providence, RI: American Mathematical Society, 1997
15. Manickam, O., Homsy, G.M.: Fingering instabilities in vertical displacement flows in porous media. J. Fluid. Mech. **288**, 75–102 (1995)
16. Otto, F.: Evolution of microstructure: an example. In: *Ergodic theory, analysis, and efficient simulation of dynamical systems*, Berlin: Springer, 2001, pp. 501–522
17. Otto, F.: Cross-over in scaling laws: a simple example from micromagnetics. In: *Proceedings of the International Congress of Mathematicians*, Vol. **III** (Beijing, 2002), Beijing: Higher Ed. Press, 2002, pp. 829–838
18. Saffman, P.G., Taylor, G.: The penetration of a fluid into a porous medium or Hele-Shaw cell containing a more viscous liquid. Proc. Roy. Soc. London. Ser. A **245**, 312–329 (1958) (2 plates)
19. Tanveer, S.: Surprises in viscous fingering. J. Fluid. Mech. **428**, 511–545 (2000)
20. Wooding, R.A.: Growth of fingers at an unstable diffusing interface in a porous medium or Hele-Shaw cell. J. Fluid. Mech. **39**, 477–495 (1969)
21. Ziemer, W.P.: Weakly differentiable functions. Berlin-Heidelberg-NewYork: Springer-Verlag, 1989

Communicated by P. Constantin